Chinese Chemical Letters 34 (2023) 107604

Contents lists available at ScienceDirect

Chinese Chemical Letters

journal homepage: www.elsevier.com/locate/cclet

Rational design of a turn-on fluorescent probe for visualization of GRP78 protein in tumor models

Ying Wen[a], Ning Jing[a], Fangjun Huo[b], Caixia Yin[a,*]

[a] Institute of Molecular Science, Key Laboratory of Chemical Biology and Molecular Engineering of Ministry of Education, Shanxi University, Taiyuan 030006, China

[b] Research Institute of Applied Chemistry, Shanxi University, Taiyuan 030006, China

ARTICLE INFO

Article history:
Received 8 March 2022
Revised 8 June 2022
Accepted 9 June 2022
Available online 14 June 2022

Keywords:
Glucose-regulated protein 78
Fluorescence probe
Living cell imaing
Tumor diagnosis

ABSTRACT

Fluorescence image for accurate tumor label still faces challenges in cancer detection and diagnostics. Emerging evidence is indicating that glucose-regulated protein 78 (GRP78), a stress-inducible protein chaperone, is a great potential biomarker and therapeutic target for cancer. However, currently available probe for image tumor based on GRP78 has not been reported, owning to no obvious strategy in probe design towards this protein. In this paper, a hairpin-shaped peptidyl probe (pepFAM) conjugated with a 5-FAM fluorophore and a dabcyl quencher at both ends was developed, respectively. The probe was designed by performing a traditional fluorescence resonance energy transfer mechanism and employing a GRP78 specifically-binding peptide. Furthermore, the probe was used to specifically image cancer cells, and accurately image xenograft tumors in mice models. The novel fluorescent probe is expected to be a useful tool for the diagnostics of cancer.

Accurate cancer imaging is essential for patient assessment, before, during, and after treatment [1]. It is most challenging at the very early stages of cancer. Thus, many advanced molecular imaging approaches including magnetic resonance imaging (MRI), computed tomography (CT), positron-emission tomography (PET), single-photon emission computerized tomography (SPECT), fluorescence imaging, photoacoustic imaging, and multimodal imaging are under constant development to improve diagnosis and to assess therapeutic efficacy [2–6]. As for accurate imaging systems, cancer imaging agents should specifically locate the target to enhance the image contrast at the tumor site [7,8]. This requires targeting ligands to bind to receptors expressed specifically on cancer cells.

The glucose-regulated protein, GRP78 (also referred to as BiP or heat shock protein family A member 5 [HSPA5]), is a stress-inducible molecular chaperone that is evolutionarily conserved from yeast to humans [9]. It is also a member of the HSP70 family. In its inactive state, GRP78 maintains endoplasmic reticulum (ER) stress sensors and ER-associated proapoptotic machineries by sustaining ER protein folding capacity to regulate the balance between cancer cell survival and apoptosis [10]. Although GRP78 was believed to reside exclusively in the ER lumen, new studies demonstrate that it can be actively translocated to the cell surface [11]. Furthermore, a wealth of literature has confirmed that GRP78 exists on the cell surface of certain cell types and functions as a multifunctional receptor to influence tumor cell growth and survival [12]. Emerging evidence has highlighted cell surface GRP78 is associated with increased malignant behavior and resistance to chemotherapy and radiotherapy by endowing various cancer cells with increased proliferative ability, altered metabolism, improved survival, and augmented invasive and metastatic potential [13]. GRP78 is, therefore, may be an effective target for cancer diagnosis and treatment [13–17]. However, currently available probes designed based on GRP78 for specifically image tumor have not been reported.

It is noted that many different synthetic peptides have been designed for GRP78 binding [18]. The specific peptide WIFPWIQL is the most employed peptide that have shown superior targeting activity and specificity towards GRP78 [19–21]. Thus, in this paper, we employed this peptide to design a fluorescent probe to specifically label GRP78 for accurate tumor fluorescence imaging. Compared to other imaging techniques, fluorescence imaging has shown unique advantages, involving real-time, multi-level, non-invasive, and non-disruptive features [1,22–25]. Our group have designed a lot of fluorescent probes towards bioactive small molecule with the excellent property [14,26–28].

In this probe design, FRET (fluorescence resonance energy transfer) design mechanism was introduced. As we know, in a

* Corresponding author.
E-mail address: yincx@sxu.edu.cn (C. Yin).

https://doi.org/10.1016/j.cclet.2022.06.027
1001-8417/

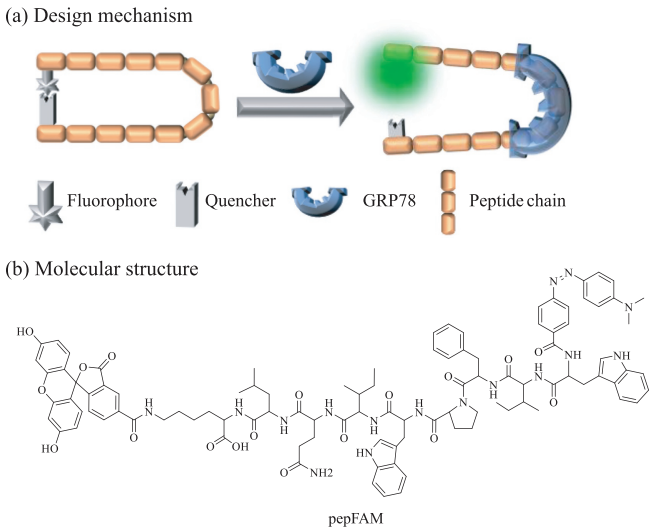

Fig. 1. Design mechanism and molecule structure of pepFAM.

probe based on FRET, a key process that affects the fluorescent signal release mainly depends on the spectral matching and distance between fluorophores, involving in donor and acceptor/quencher [23,27,29]. The peptide chain above described has outstanding advantages, such as small size, little immunogenicity, and economic synthesis; offers an ideal linker for donor and quencher of probes. Thus, both sides of this peptide were conjugated with classic FRET fluorophore molecular pairs: 5-FAM fluorophore and dabcyl quencher, respectively. Due to the flexibility of peptide chain and π-π stacking of dyes, the whole probe showed a hairpin shape; the FRET process happened and the fluorescent signal of 5-FAM was quenched (Fig. 1a). After the response to GRP78, the conformational changes lead to increase in the space distance of fluorophore and quencher, suppression of FRET process, and finally release of fluorescence of 5-FAM (Fig. 1a). The produced fluorescence signal was used to detect the presence of GRP78 with high sensitivity and high selectivity. Furthermore, the capacity of specifically image cancer cells and tumors of this probe was verified.

The details of synthesis and characterization of probe (designated as pepFAM, shown in Fig. 1b) are provided in the Experiments Section and Figs. S1 and S2 (Supporting information). The spectroscopic properties of pepFAM were assessed under *in vitro* physiological conditions (in PBS, pH 7.4). In the absence of GRP78, pepFAM displayed weak fluorescent emission under excitation of 490 nm (Fig. 2a). After the addition of GRP78, a green fluorescence majored at 530 nm increased over time, as shown in Fig. 2a. Fig. 2b showed the absence spectra of pepFAM. Upon the addition of GRP78, the absorbance majored at 490 nm increased slightly. To verify the selectivity of pepFAM for GRP78, the fluorescent changes were examined upon addition of intracellular proteins (glutathione *S*-transferases, human albumin, lysozyme, and ferritin), active sulfur (Cys, Hcy and GSH), reactive oxygen species (H_2O_2) and ions ($NaHSO_3$, NaF, NaCl and $NaHCO_3$). At 2 h, the above species induced a weak increase with fluorescence intensity at 530 nm being (<2.4-fold), which was markedly smaller than that obtained with GRP78 (9.7-times), as shown in Fig. 2c. The good selectivity showed that pepFAM could serve as a turn-on fluorescent probe for GRP78 with minimum interference from other ROS/RSS, proteins or ions. In addition, a linear correlation between the fluorescent emission intensity at 530 nm and the GRP78 concentration was presented at Fig. 2d. The detection limit of the probe for GRP78 was calculated with the equation $3\sigma/k$ [30]. The value was estimated as 0.19 μg/mL. In $3\sigma/k$, σ is the standard deviation of blank measurement; k is the slope of the calibration curve in Fig. 2d. Fluorescence kinetics tests of probe and probe for GRP78 have been performed and displayed in Fig. S3 (Supporting information). These data indicated that pepFAM is an ideal turn-on probe for GRP78 with high selectivity and high sensitivity.

Next, CCK-8 assay was performed to verify the low acute toxicity of pepFAM to living HCT116 cells (human colorectal cancer

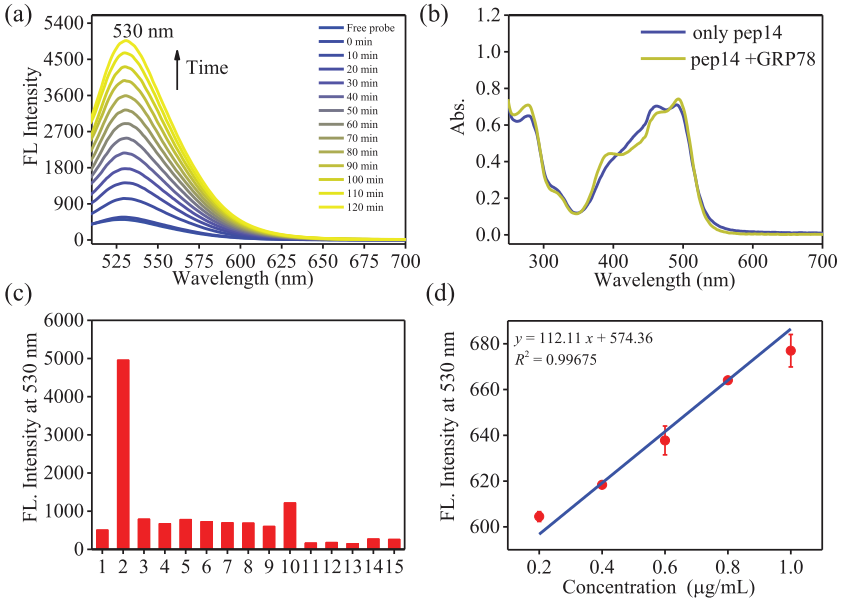

Fig. 2. (a) Fluorescence spectral change of pepFAM (5 μmol/L) upon addition of GRP78 (50 μg/mL) in PBS (pH 7.4), λ_{ex} = 490 nm, slit: 5 nm/5 nm. (b) Absorption spectra of pepFAM (5 μmol/L) without or with GRP78 (50 μg/mL). (c) Selectivity test of pepFAM (5 μmol/L) towards GRP78 activity over other related biological species and enzymes. 1 to 15 represents free probe, upon additional of GRP78 (50 μg/mL), Cys (1 mmol/L), GSH (1 mmol/L), HCy (1 mmol/L), GSTs (50 μg/mL), human albumin (50 μg/mL), lysozyme (50 μg/mL), H_2O_2 (1 mmol/L), ferritin (50 μg/mL), $NaHSO_3$ (200 μmol/L), NaF (200 μmol/L), NaCl (200 μmol/L), $NaHCO_3$ (200 μmol/L), and $NaNO_2$ (200 μmol/L), respectively. (d) Plot of fluorescence intensity at 530 nm for pepFAM (5 μmol/L) *vs.* [GRP78] in the range of 0.2~1.0 μg/mL. Fluorescence intensity values at 530 nm of pepFAM were obtained after incubation GRP78 with different concentration at 37 °C in PBS buffer after 2 h. The error bars and average values were shown for independently repeated 3 times experiments.

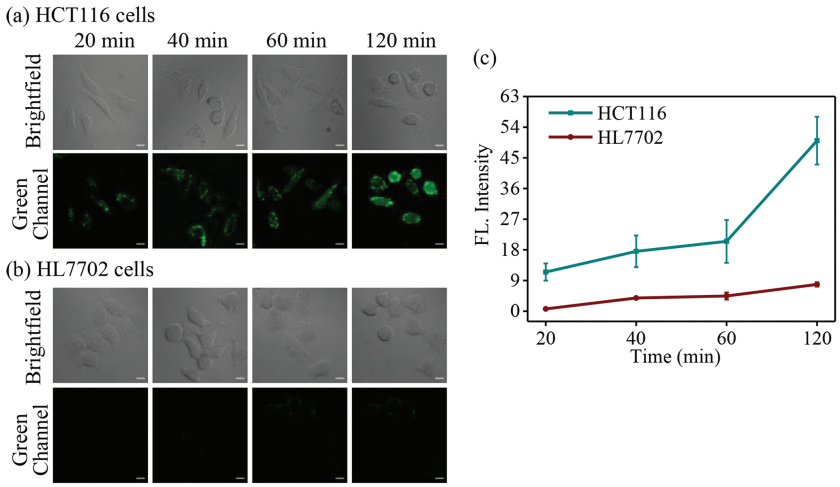

Fig. 3. CLSM imaging with pepFAM in (a) HCT116 and (b) HL7702 cells. Green channel (λ_{ex} = 488 nm, λ_{em} = 500-560 nm) imaging signal of cells preincubated with pepFAM (10 μmol/L) were collected for 20, 40, 60, and 120 min. Scale bar = 10 μm. (c) Corresponding average fluorescence intensities of green channel in (a) and (b), error bars are ± S.D.

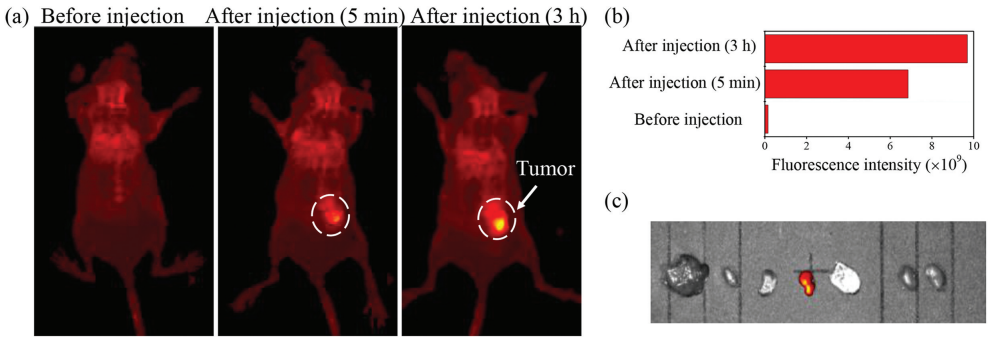

Fig. 4. (a) *In vivo* imaging of pepFAM (2 mmol/L) in HCT116-bearing nude mice at 0, 5, and 180 min. Green channel: λ_{ex} = 465 nm, λ_{em} = 520–580 nm. (b) Corresponding fluorescence intensities of mice in tumor region (white circles in (a)). (c) Fluorescence imaging of isolated organs (liver, heart, spleen, tumor, lung, kidney, from left to right, respectively).

cells). The viabilities were shown to be >88.7% at 12 h in the incubation of 1–20 μmol/L pepFAM (Fig. S4 in Supporting information), clearly suggesting probe has low acute toxicity and excellent biocompatibility. Then, confocal imaging experiments were employed to evaluate the capabilities of probe to permeate living cells and specifically turn on cancer cells. HCT116 cells were incubated with 10 μmol/L pepFAM. As shown in Fig. 3a, the green channel signal dramatically increased over time and corresponding fluorescence intensity increased by 4.4-fold at 120 min, in Fig. 3c. The time-dependent green fluorescence increase was attributed to the increase of incubation time of probe and the specific response of probe for GRP78. It is noted that the green channel signal is almost undetectable in HL7702 cells (human normal liver cells), even with 2 h incubation time (Figs. 3b and c). This data indicated that the probe can specifically turn on cancer cells.

To verify the capacity of the probe to for specifically tumor labeling, a tumor model was established by subcutaneous injection of HCT116 cells in the right-back of a BALB/c nude mouse at the age of 6–8 weeks. The mice were kept for about 2 weeks. Then fluorescent imaging of the mice was performed using a small animal optical imaging system. We obtained images of the mice after injection of the probe at 0, 5, and 180 min, which are given in Fig. 4a. Weak fluorescence at the tumor site was observed after 5 min of probe injection, indicating that the probe exhibits good tissue permeability and high sensitivity. Within 180 min of monitoring, the fluorescence signal at tumor sites in the mice became more and more obvious (Fig. 4a). At 180 min, the fluorescence intensity in the tumor region increased by 63.5-fold, compared to that of before injection (Fig. 4b). *Ex vivo* fluorescence images of the isolated organ assay displayed that the obvious fluorescence signal appeared in the tumor, instead of other organs, including the heart, liver, kidneys, spleen, and lung (Fig. 4c).

In summary, this paper described the design and synthesis of a turn-on fluorescent probe and its excellent properties, as well as their application in solution, in living cell, and *in vivo* tumor imaging. The probe is composed of a specific peptide chain for GRP78 protein conjugated with a 5-FAM fluorophore and a dabcyl quencher based on FRET mechanism to form harpin-shape structure. The probe could specifically recognize GRP78 protein, open the harpin structure and release green fluorescence. Favourable characteristics of the probe also are demonstrated in terms of high specificity, high sensitivity, and stable photo-stability. In particular, the probe has been successfully applied to cellular imaging and the diagnosis of tumors in a xenogeneic mouse model. The superior properties of the probe give it great potential in other biosystems and *in vivo* imaging studies.

Declaration of competing interest

The authors declare no competing financial interest.

Acknowledgments

We acknowledge the National Natural Science Foundation of China (Nos. 21705102, 21775096, 22074084) and the Basic Research Program of Shanxi Province (Free Exploration) (No.

20210302123430). We are also very grateful for the help of Dr. Lichao Zhang. All the animal experiments were performed by following the protocols approved by the Radiation Protection Institute of Drug Safety Evaluation Center in China (Production license: SYXK (Jin) 2018-0005).

Supplementary materials

Supplementary material associated with this article can be found, in the online version, at doi:10.1016/j.cclet.2022.06.027.

References

[1] M. Gao, F. Yu, C. Lv, J. Choo, L. Chen, Chem. Soc. Rev. 46 (2017) 2237–2271.
[2] K.I. Matsumoto, J.B. Mitchell, M.C. Krishna, Molecules 26 (2021) 1614.
[3] S.H. Gardner, C.J. Reinhardt, J. Chan, Angew. Chem. Int. Ed. 60 (2021) 5000–5009.
[4] J. Liu, M. Liu, H. Zhang, W. Guo, Angew. Chem. Int. Ed. 60 (2021) 12992–12998.
[5] X. Zhang, Y. Chen, H. He, et al., Angew. Chem. Int. Ed. 60 (2021) 26337–26341.
[6] Z. Zhao, C.B. Swartchick, J. Chan, Chem. Soc. Rev. 51 (2022) 829–868.
[7] L. Wu, X. Qu, Chem. Soc. Rev. 44 (2015) 2963–2997.
[8] Y. Wen, C.L. Schreiber, B.D. Smith, Bioconjug. Chem. 31 (2020) 474–482.
[9] I. Hernandez, M. Cohen, Cancer Lett. 524 (2022) 1–14.
[10] M. Wang, S. Wey, Y. Zhang, R. Ye, A.S. Lee, Antioxid. Redox Signal. 11 (2009) 2307–2316.
[11] I.M. Ibrahim, D.H. Abdelmalek, A.A. Elfiky, Life Sci. 226 (2019) 156–163.
[12] U. Gopal, S.V. Pizzo, J. Cell. Physiol. 236 (2021) 2352–2363.
[13] M. Farshbaf, A.Y. Khosroushahi, S. Mojarad-Jabali, et al., J. Control. Release 328 (2020) 932–941.
[14] Y. Huang, Y. Zhang, F. Huo, et al., J. Am. Chem. Soc. 142 (2020) 18706–18714.
[15] R.J. Passarella, D.E. Spratt, A.E. van der Ende, et al., Cancer Res. 70 (2010) 4550–4559.
[16] M. Gonzalez-Gronow, U. Gopal, R.C. Austin, S.V. Pizzo, IUBMB Life 73 (2021) 843–854.
[17] S. Xia, W. Duan, W. Liu, X. Zhang, Q. Wang, J. Transl. Med. 19 (2021) 118.
[18] Y.L. Tsai, A.S. Lee, Cell surface GRP78: anchoring and translocation mechanisms and therapeutic potential in cancer, in: S.V. Pizzo (Ed.), Cell Surface GRP78, a New Paradigm in Signal Transduction Biology, Academic Press, New York, 2018, pp. 41–62.
[19] M.A. Arap, J. Lahdenranta, P.J. Mintz, et al., Cancer Cell 6 (2004) 275–284.
[20] A.N.I. Viswanath, J.W. Lim, S.H. Seo, et al., Chem. Biol. Drug Des. 92 (2018) 1555–1566.
[21] Z. Li, C. Zhao, Z. Li, et al., Int. J. Biochem. Cell Biol. 47 (2014) 68–75.
[22] P. Wei, L. Liu, Y. Wen, et al., Angew. Chem. Int. Ed. 58 (2019) 4547–4551.
[23] X. Wu, R. Wang, N. Kwon, H. Ma, J. Yoon, Chem. Soc. Rev. 51 (2022) 450–463.
[24] Y.F. Huang, Y.B. Zhang, F.J. Huo, Y. Wen, C.X. Yin, Sci. China Chem. 63 (2020) 1742–1755.
[25] L. Liu, F. Liu, D. Liu, et al., Angew. Chem. Int. Ed. 61 (2022) e202116807.
[26] W. Zhang, F. Huo, F. Cheng, C. Yin, J. Am. Chem. Soc. 142 (2020) 6324–6331.
[27] Y. Wen, F. Huo, J. Wang, C. Yin, Anal. Chem. 91 (2019) 15057–15063.
[28] Y. Wen, F.J. Huo, C.X. Yin, Chin. Chem. Lett. 30 (2019) 1834–1842.
[29] E. Pazos, O. Vazquez, J.L. Mascarenas, M.E. Vazquez, Chem. Soc. Rev. 38 (2009) 3348–3359.
[30] Y. Wen, F. Xue, H. Lan, et al., Biosens. Bioelectron. 91 (2017) 115–121.